IEEE Access
Multidisciplinary | Rapid Review | Open Access Journal

Received August 3, 2020, accepted August 10, 2020, date of publication August 24, 2020, date of current version September 9, 2020.

Digital Object Identifier 10.1109/ACCESS.2020.3018870

Uncertainty Sources in the Estimation of the Partial Discharge Inception Voltage in Turn-to-Turn Insulation Systems

MANUEL GÓMEZ DE LA CALLE[1], JUAN MANUEL MARTÍNEZ-TARIFA[2], (Senior Member, IEEE), ÁNGEL MANUEL GÓMEZ SOLANILLA[2], AND GUILLERMO ROBLES[2], (Senior Member, IEEE)

[1]Electrical and Light Department, Airbus Defence and Space, 28906 Madrid, Spain
[2]Department of Electrical Engineering, Universidad Carlos III de Madrid, 28911 Madrid, Spain

Corresponding author: Manuel Gómez de la Calle (manuel.g.delacalle@airbus.com)

ABSTRACT Partial discharges (PD) are one of the main causes of premature failure in low-voltage motors driven by variable-speed drives. The use of these control systems are being quite extended due to new applications, such as the more electric aircraft (MEA) or hybrid and electric vehicles, and this has pushed research towards appropriate designs of electric motors to avoid, as much as possible, the presence of PD within their windings. This article presents a model to predict the partial discharge inception voltage (PDIV) in the insulation of low-voltage machines. A value for the secondary ionization coefficient based on a statistical study is also proposed. The deviations of the model are also studied by obtaining the uncertainty of the value of that coeficient and the predicted values of the PDIV for a set of wires. This uncertainty will be compared with other error sources such as generator harmonics and humidity. Finally, the tests are done for different temperatures extend the model applicability.

INDEX TERMS Insulation design, inverter-fed machine, partial discharges, Paschen's law, temperature, Townsend's coefficients.

I. INTRODUCTION

The new widespread applications for electric mobility is extending the trend to control speed and torque of squirrel cage induction motors in an efficient way [1], [2]. However, these variable speed drives (VSD) have changed the electrical stresses [2]–[6] making turn to turn insulation systems the weakest point of these low-voltage (LV) machines. The high electrical fields applied to some microns of enamel whose design was for a different purpose [6]–[8], cause the appearance of partial discharges (PD). It is believed that these insulation problems are responsible for a high rate of unexpected failures [9]–[12]. All these reasons justify the research trends towards designs of new low-voltage motors for VSD applications, where the probability of PD should be reduced as much as possible [13]. On this purpose, accurate models for assessment of partial discharge inception voltage (PDIV) are needed to design the insulation system.

The associate editor coordinating the review of this manuscript and approving it for publication was Atif Iqbal.

The authors of [6] studied the breakdown mechanism in parallel-wound wires, using experimental results and Paschen's Law to analyze the impact of different parameters such as the insulation design or temperature. The model calculation is not clearly specified, in contrast to [14], whose authors used a finite element method (FEM) to compute the electric field lines for different potentials, and determined the inception voltage based on the comparison with those given by Paschen's Law for parallel conductors. A similar approach is followed by [15], but enhancing the model using an IEEE standard test object (motorette) for the experimental results and presenting a more complete model that comprises FEM simulations combined with Paschen's Law modified to include the temperature effect.

By contrast, authors of [17] question the validity of Paschen's Law for PDIV prediction in turn to turn insulation systems, as the electric fields created by the coils are non-uniform. They used the streamer criterion to predict the PDIV (without including the impregnation varnish), changing the air density to include the effects of temperature in the proposed model.

From the references reviewed in the present literature it is clear that there is much uncertainty around the estimation of the secondary ionization coefficient. This coefficient helps to calculate the effective ionization of a volume of air due to the action of an electrical field. There isn't yet any proposal for a systematic way to estimate this parameter, which plays a key role in the PDIV prediction models.

The approach followed in this article is to combine Paschen's Law in gases [6], [14], [15] with the finite element method to calculate the ionization distance [14], [15], in a twisted pair geometry to predict the PDIV in motor coils. The originality of the study is to use constant-field lines in turn to turn insulation systems instead of electric-field lines. In addition, the influence of the secondary ionization coefficient value on the prediction model will be deeply studied. The outcome of this analysis will be a model for partial discharge inception voltage prediction in turn to turn insulation systems. The effect of several variables on the quality of the prediction made by the model has also been analyzed: the difference between the theoretical and experimental instantaneous inception voltage, temperature and moisture, with special focus on the errors created by the estimation of the secondary ionization coefficient. The model will be applied to the calculation of the PDIV at ambient and rated temperatures of electric motors, so the tests would simulate changes of load.

II. PHYSICS OF PARTIAL DISCHARGE INCEPTION VOLTAGE

The prediction of partial discharges inception voltages is always based on the calculation of the applied fields within all insulation systems and the modelling of the ignition conditions for PD occurrence. If the applied electric field equals the inception field in any analyzed volume, then, the PDIV has been reached. Due to the uneven voltage distribution through turns of these VSD motors, nearly the whole voltage will be applied to only a few enamel micrometers [4]. As the final goal of the experiment is to study the PDIV of turn-to-turn insulation, a twisted pair layout was chosen, because it is advised as one of the sample types for turn-to-turn insulation tests in the literature [16]. This setup allows a continuous contact between wires, similar to the worst-case scenario in low-voltage electric machine windings, which is often the weakest insulation subsystem for inverter-fed motors [8].

To calculate the applied fields with FEM, the geometric and permitivity (see [17]) data from several magnet wires shown in Table 1 are used.[1]

In the simulation, no solid insulation is assumed within the air wedge between the magnet wires, which is considered a good approach since it is a worst-case scenario (bad impregnation in the windings) appropriate for a conservative design. The modelling of the ignition conditions for PD occurrence has been done through different approaches in the past. The majority of previous studies use Paschen's Law for

[1]The * is a tag to distinguish between the two magnet wires with diameter 0.6 mm.

TABLE 1. Characteristics of the cooper cables under test.

Magnet wire diameter [mm]	Enamel thickness [μm]	Dielectric Permittivity [-]
0.4	16	4.53
0.6	18	3.87
0.6*	30	3.99
0.8	24	3.74
1.0	30	4.09
1.2	42	3.60
1.8	43	3.56

the calculation of the inception field [6], [14], [15]:

$$E = \frac{U}{d} = \frac{B \cdot P}{\ln\left(\frac{A \cdot P \cdot d}{k}\right)} \tag{1}$$

Being E the applied electric field, U the breakdown voltage, P the pressure, d the gap distance, k:

$$k = \ln\left(1 + \frac{1}{\gamma}\right), \tag{2}$$

and γ the Townsend's secondary emission coefficient, which represents the average number of electrons released from the cathode per incident positive ion [18]. The parameters A and B depend on the gas composition and are found to be constant over a range of $\frac{U}{d}$.

However, the application of this equation has several limitations:

1) Paschen' Law is based on a specific simplification of Equation 3

$$\int_0^d \alpha'(x) \cdot dx = \ln\left(1 + \frac{1}{\gamma}\right) \tag{3}$$

where x is the path along the line defined by a constant electric field. Under this assumption, the effective first ionization phenomena $\alpha' = \alpha'(x)$ (accounting for ionization and recombination rate) is considered constant within the inter-electrode distance d, because the applied electric field E is assumed constant within the analyzed air volume (in the generalized model, $\alpha' = \alpha'(x, E, P)$, being P the pressure). This simplification cannot be assumed for this geometry [18], so the path followed by the electric field lines (the lines that would define the path followed by a free electron) cannot be used in the line integral in Equation 3.

2) Equation 3 is based on Townsend ionization mechanism, whereas the streamer inception mechanism has proven to be effective in previous works [17]. In that case, Equation 3 can be rewritten as:

$$\int_0^{x_c} \alpha'(x) \cdot dx = \ln(N_c) \tag{4}$$

Being N_c the critical concentration of ions at an inter-electrode distance x_c ($x_c < d$) enough to create the avalanche starting the streamer. Classical studies have given a value of 10^8 for this parameter in air, whereas other values have been proposed in previous works [17], [18] or it has even been made variable with pressure and distance [19].

3) The Townsend's secondary ionization coefficient γ value is well known for metal electrodes [18], but when covered with epoxy resins, the γ value [14], [15] is not quite clear. It is stated that this electron emission is unlikely [17] because the work function of a dielectric insulator is higher (around double) than that of many metals. However, the electric fields needed for inception in these non-uniform fields applications are much higher than 3 kV/mm (typical for air for uniform fields), which, for the dozens of microns of distances involved can lead to higher kinetic energy for the electrons which impact on the resin surface [6], [15].

This article analyzes under which circumstances Paschen's Law can be used to predict the partial discharge inception voltage in a non-homogeneous applied field application such as turn to turn insulation systems with enameled magnet wires. Once the applied voltage reaches the PDIV, the electron avalanche will follow the electric field lines, which are perpendicular to the equipotential surfaces. This path has been used in previous works [6], [15] as the distance gap d in Paschen's Law to determine the PDIV. This approach is not quite accurate as Paschen's Law assumes constant electric field magnitude along the analyzed lines. Therefore, the authors have discarded the use of the electric field lines from the analysis, as they are not appropriate to apply Paschen's Law to this geometry. The presented proposal can be used to estimate the iginition of discharges, but not the path followed by electron avalanches within the gas nor the localization of volumes affected by ionization.

III. FEM MODELLING AND CALCULATION

A simplified FEM analysis of the electrical field created by the twisted pair was carried out. The laboratory free space is modelled as a semi-circle of 1 m radios filled with air and the laboratory floor is modelled as the ground plane with 0 V.

The twisted pair are represented as two circular conductors, separated and enclosed by an insulating layer of enamel, resting on a dielectric base represented as a rectangle of 2 cm high and 20 cm wide ($\varepsilon_{r\,\max}$=2.5), which is over the ground plane. The dielectric permitivity value of each enamel wire is extracted from Table 1.

The mesh chosen for the FEM simulation is a key parameter that strongly affects the accuracy of the model. The electron avalanche is created by the electric field present in the air wedge between the wires. This is why, the mesh has been refined in this area, to obtain a reliable and detailed value of the electric fields in this air area. The mesh used for all the simulations is illustrated in Figure 1.

The results of the FEM model designed are shown in Figure 2. After each FEM simulation, the points of the volume (4000×4000 points in the air wedges) where the electric field magnitude is constant have been analyzed (see Figure 3).

To compare the applied electric field lines (all the lines from Figure 3) to the ionization condition (1), it is necessary to know the distance d along which this electric field

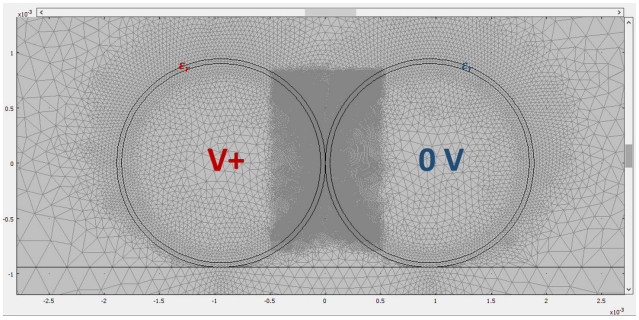

FIGURE 1. View with the conductors and the mesh choosen.

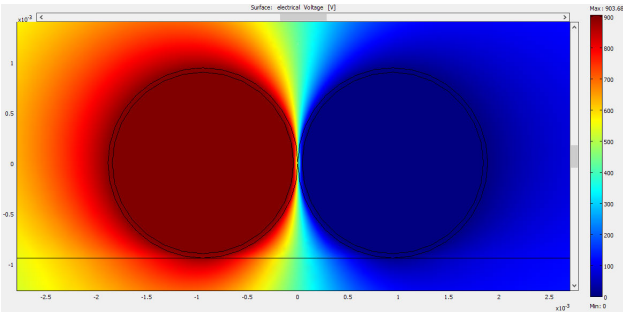

FIGURE 2. FEM simulation result for wires with ϕ1.8 mm and 43 μm insulation thickness.

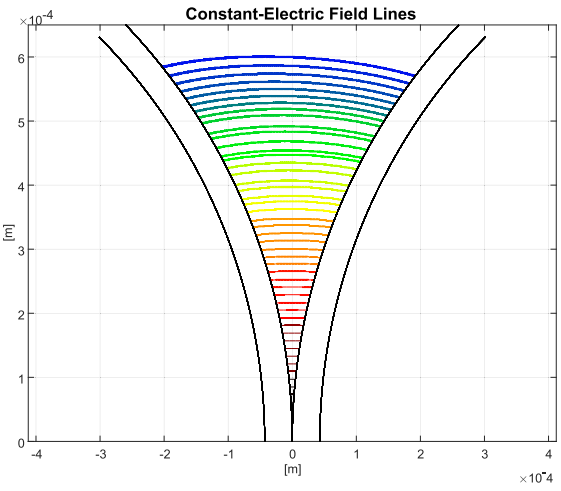

FIGURE 3. Constant-electric field lines obtained for wires with ϕ1.8 mm and 43 μm insulation thickness.

is applied. This has been done through an adjustment of the points where the electric field has a fixed value to a specific function based on second-order polynomials, see Figure 4. They fit the constant electric field line with a Pearson's correlation coeffient of $r > 0.98$ for all the adjustments. The value of the distance d is calculated as the line integral of the adjusted polynomial between two points.

Once the constant-electric field lines are obtained from the simulations,[2] they have been represented as a function of their length in the air-gap between wires. The results show an expected reduction of the applied fields with d (see Figure 5).

[2]It should be noted that constant-electric field lines are not perpendicular to the equipotential surfaces as electric field lines are.

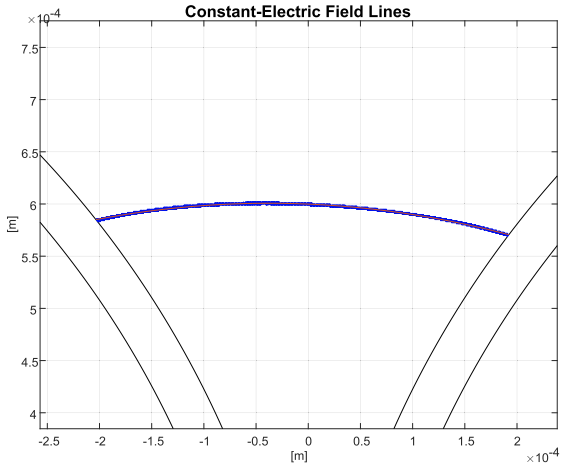

FIGURE 4. Adjustment to a constant-field (2.2 kV/mm) line in ϕ1.8 mm with 43 μm insulation thickness.

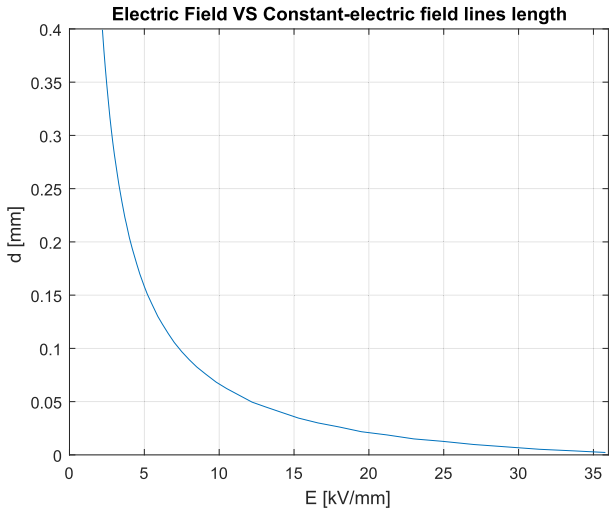

FIGURE 5. Electric field within the air wedge of Figure 3 as a function of its constant-electric field line distance. ϕ1.8 mm with 43 μm insulation thickness.

The analysis is restricted to fields above 2.2 kV/mm, since this magnitude seems to be low enough for discharge ignition (which will be confirmed from the results later on) and also for distances above 6 μm, since below this value Paschen's Law is not valid [20].

In the Section V, the authors will compare these curves simulated with experimental PDIV values with those from Equation 1, to check if the ionization condition is reached (that is, whether both curves cross at any distance d).

Regarding the second ionization coefficient, given the difficulty to obtain reliable and concrete information, the authors follow a similar experimental approach as in [17]. The experimental PDIV results will be used to compare applied field magnitudes to condition (1) to obtain a function with different values of k, which is directly related to γ by the Equation 2. The next step is to analyze how this value changes for different wires (from different manufacturers), and which error arises if an average value is used for the PDIV prediction. Finally, the k estimation at room temperature will

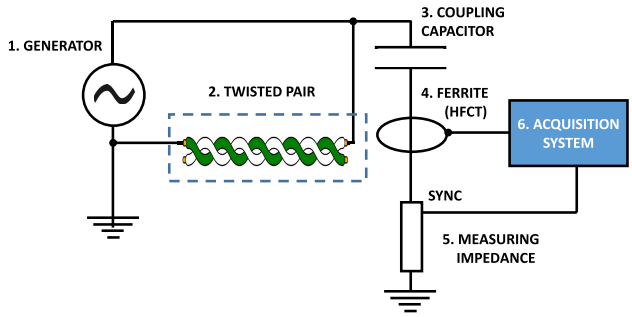

FIGURE 6. Test circuit components for PD detection.

be used for the prediction at different temperature levels to account for different environmental and load conditions of electric machines.

IV. EXPERIMENTAL PROCEDURE

The testing circuit is detailed in Figure 6. The generator is a 50 Hz variable sinusoidal voltage source (GLP1-e HV by Schleich) which allows to control the applied RMS (Root Mean Square) voltage. Each twisted pair is connected as specified in Figure 6: one of the terminals to the high voltage output of the source, and the other one to the circuit ground. This connection simulates the maximum applied voltage to the turn-to-turn insulation system of LV electric machines.

This is a normalized detection circuit according to [13]. The circuit uses a low impedance (coupling capacitor and measurement impedance) path to detect partial discharge pulses with high frequency components. As shown in Figure 6, the pulses are sensed with a High Frequency Current Transformer (HFCT) and visualized using a commercial acquisition system. In our laboratory, this instrumentation arrangement guarantees the detection of PD events with magnitudes lower than 5 pC, so the system sensitivity is appropriate to detect the ignition of discharges accurately. In the case of having a measuring system with a lower sensitivity, the detection of the PDIV will affect the model. This equipment allows us to visualize the partial discharge pattern synchronized with the generator voltage and the pulses waveforms.

The criteria used for the measurement of the PDIV is the lowest peak voltage to maintain a self-sustaining process of ionization; in other words, the lowest voltage to have repetitive partial discharges in the acquisition system. This was measured observing the phase-resolved partial discharge (PRPD) patterns and the pulse waveshapes in the commercial acquisition system (see Figure 7).

For each wire diameter, 10 samples were tested to obtain statistically reliable data. To avoid errors from manual changes in the applied voltage, the source was programmed to increase its voltage in an automatic way with rate of rise of 6 V/s. For each sample, the ignition voltage is measured 3 times and averaged to obtain the PDIV value.

V. EXPERIMENTAL RESULTS

The partial discharge mechanism is a stochastic phenomenon which is well fitted using a two-parameter Weibull

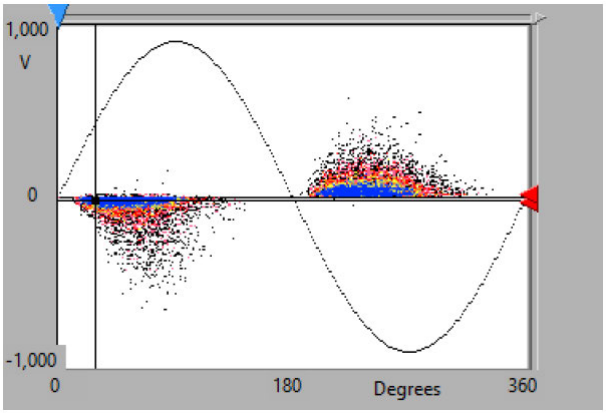

FIGURE 7. PRPD pattern for PDIV at ϕ1.8 mm with 43 μm insulation thickness at room temperature. Nw=37.3, Qmax=2 pC y Trigger level=10 mV.

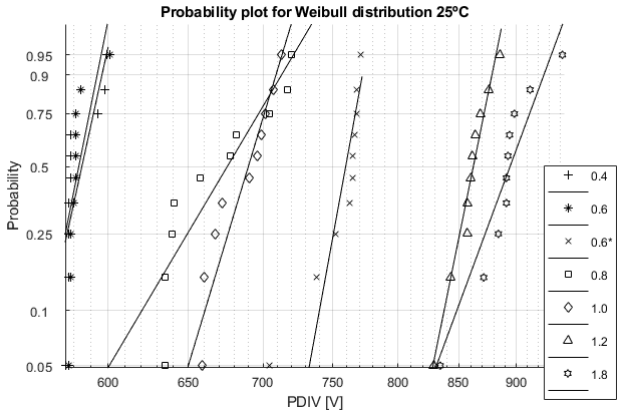

FIGURE 8. Weibull probability plot for different PDIV values for all the magnet wires tested at 25°C.

distribution [16], [17]. For a generic variable v, the cumulative distribution is detailed in Equation 5.

$$P(v) = 1 - e^{-(v/\alpha)^{\beta}} \tag{5}$$

where α is the scale parameter of v ($P(v = \alpha) = 0.6321$) and β is the shape parameter, the higher this value is, the less dispersed the distribution is. In Table 2, Table 3 and Table 4 the scale (PDIV) and shape parameters are reported for the tests performed at 25°C,[3] 110°C and 150°C, in addition with the testing environmental conditions.[4] In addition to the tables, the Weibull probability plot is shown in Figure 8 for the 25°C data recorded, to visually determine if the data comes from a Weibull distribution.

The high values for beta shows that the scale factor parameter is quite a good estimator for the studied variable. In the past work [17] it was demonstrated that PDIV has a strong dependence on enamel thickness and weak on wire diameter. In addition, lower PDIV values are detected for higher temperatures, a trend previously observed in [15], [17], [21].

[3]These measurements were performed in a laboratory with a controlled temperature around 25°C.

[4]Notice that the humidity column does not appear in Table 3 and Table 4, because all the water has completely evaporated.

TABLE 2. Weibull fitted distribution statistical values for testing at 25°C temperature.

Wire [mm]	Enamel [μm]	PDIV$_{PEAK}$ [V]	β [-]	Pressure [hPa]	Humidity [%]
0.4	16	588.31	52.53	1025.6	36.5
0.6	18	586.90	67.18	1014	45
0.6*	30	766.50	35.92	1016	44
0.8	24	687.31	20.13	1025.6	36.5
1.0	30	695.79	36.54	1014.3	34
1.2	42	866.91	59.08	1020	46
1.8	43	903.68	34.01	1020	32

TABLE 3. Weibull fitted distribution statistical values for testing at 110°C.

Wire [mm]	Enamel [μm]	PDIV$_{PEAK}$ [V]	β [-]	Pressure [hPa]
0.4	16	513	47.37	1013.3
0.6	18	557	62.17	1018.0
0.6*	30	701	152.33	1003.3
0.8	24	632	48.66	1010.0
1.0	30	697	189.22	1007.7
1.2	42	830	65.82	1012.4
1.8	43	851	57.35	1003.0

TABLE 4. Weibull fitted distribution statistical values for testing at 150°C.

Wire [mm]	Enamel [μm]	PDIV$_{PEAK}$ [V]	β [-]	Pressure [hPa]
0.4	16	519	184.84	1020.6
0.6	18	580	636.08	1020.6
0.6*	30	706	336.51	1013.8
0.8	24	649	19.52	1017.1
1.0	30	687	23.01	1017.1
1.2	42	824	60.02	1017.1
1.8	43	824	65.76	1023.4

VI. PDIV PREDICTION MODEL

A. CALCULATION OF k

Paschen's Law can describe the onset of breakdown phenomena in uniform fields, so, as explained in Section II, the constant-electric field lines obtained from the simulations will be used with this law in non-uniform fields. The pararmeter k will be estimated based on this approach and on the PDIV experimental data. This parameter k is related with the Townsend's secondary emission coefficient γ by Equation 2, as defined in [18]. With this value, gamma can be easily obtained through Equation 6.

$$\gamma = \frac{1}{e^{k} - 1} \tag{6}$$

This coefficient is used in [14] with a value of $\gamma = 0.01$ which was obtained from a previous study, while [15] uses $\gamma = 0.0004$ which has been determined by experimental measurements in the laboratory. Accordingly, researchers do not agree in a value for this coefficient.

The parameters of Equation 1 are $A = 12$ions/Torr.cm and $B = 365$V/Torr.cm, and the environmental variable P is the atmospheric pressure indicated in Table 2 to 4. $E = \frac{U}{d}$ and d values were obtained for each experimental PDIV from FEM simulations (see Figure 3 and Figure 5). The result of these calculations for each wire diameter is shown in Figure 9.

It should be reminded that only a combination of electric field and constant-electric field lines distance values fulfilled the ionization condition of Equation 1, because the

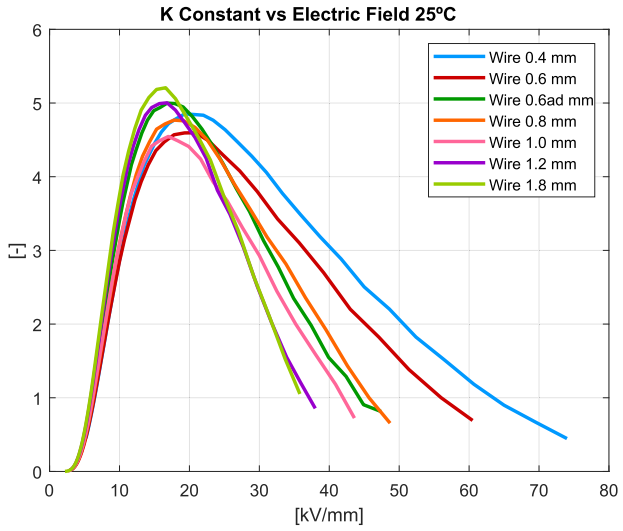

FIGURE 9. Parameter k for different electric field values for all the magnet wires tested at 25°C.

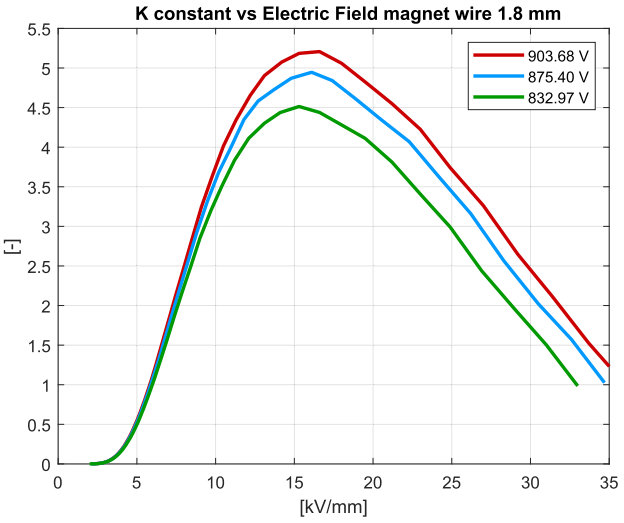

FIGURE 10. Parameter k for different voltage values ϕ1.8mm.

TABLE 5. Maximum k value for each magnet wire at 25°C.

Wire [mm]	$PDIV_{PEAK}$ [V]	km [-]
0.4	588.31	4.85
0.6	586.90	4.60
0.6*	766.50	5.00
0.8	687.31	4.77
1.0	695.79	4.55
1.2	866.91	5.00
1.8	903.68	5.21
Average		**4.86**

simulations used the lowest voltage to maintain a selfsustaining process of ionization. Therefore, the complete curves from Figure 9 cannot be used, and the greatest constrain for the ionization condition must be considered; therefore, only the maximum k value is meaningful.

This rationale is illustrated in Figure 10, where the three k curves for PDIV voltage and 20 V_{RMS} (28.28 V_{peak}) and 50 V_{RMS} (70.71 V_{peak}) below this level (1.8 mm diameter wire) are plotted. Experimentally, it is ensured that below the PDIV voltage there is no partial discharge activity and in the plots of Figure 10, none of the k values for the lower voltages reaches the maximum value of $km = 5.2$ of the PDIV. Thus, the maximum k value for each magnet (Figure 9) is presented in Table 5.

The arithmetic mean of the k maximum values of Table 5 is **4.86**, which corresponds to a γ value of **0.0078** when k is used in Equation 6. This value is greater than the 3.93 ($\gamma = 0.02$) used by [18], but lower than other values of k found in the literature: 5.61 ($\gamma = 0.01$) [14], 5.98 [17] and 7.82 ($\gamma = 0.0004$) [15].

B. PREDICTION CAPABILITY

To estimate the PDIV values using Equation 1, including the parameter k from the Table 5, the authors will follow the same process described in [14] and [15]. Different voltages were applied in the FEM model of each wire obtaining the E-d curves such as those from Figure 5; the process is

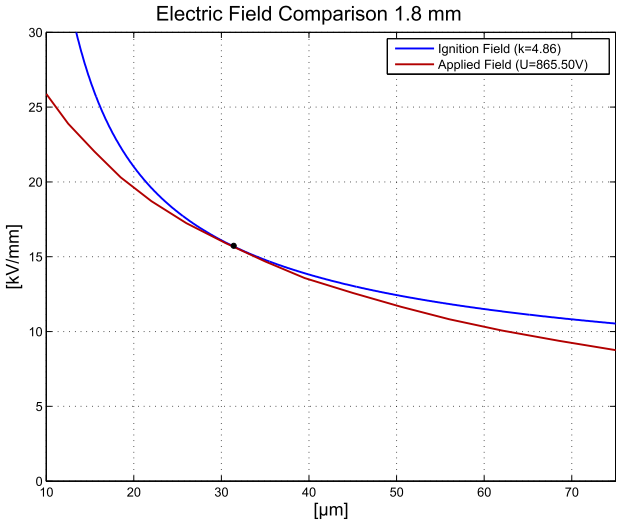

FIGURE 11. Ignition field with k=4.86 vs applied field for ϕ1.8 mm at 25°C.

finalized when one of these crosses the E-d curve from the Paschen Law. Obviously, the use of the specific km on each wire would give a perfect agreement, but the authors want to assess which error is obtained on each wire using the average km value. In Figure 11 it is shown, as an example, the intersection of Paschen's Law E-d curve (with k=4.86) with a simulated applied field E-d curve in one point. A lower applied voltage E-d curve will not cross Paschen's Law E-d curve (no ionization process), and a higher applied voltage E-d curve would cross it in two points (several ionization processes with several constant-field lines ionizing). Hence, the voltage for the E-d curve which is tangential to the Paschen's Law E-d curve would be the estimated PDIV voltage.

The process is applied to each magnet wire to estimate its theoretical PDIV. In order to analyse the influence of parameter k on the PDIV estimation accuracy, the process was performed for km_{min}=4.55, km_{avg}=4.86 and km_{max}=5.21.

TABLE 6. PDIV estimation with km_{min} at 25°C.

Wire [mm]	$PDIV_{PEAK}$ exp [V]	$PDIV_{PEAK}$ est [V]	Error %
0.4	588.31	560.03	-4.81
0.6	586.90	578.41	-1.45
0.6*	766.50	722.66	-5.72
0.8	687.31	664.68	-3.29
1.0	695.79	695.79	0.00
1.2	866.91	817.42	-5.71
1.8	903.68	834.39	**-7.67**
Average			**4.09**

TABLE 7. PDIV estimation with km_{avg} at 25°C.

Wire [mm]	$PDIV_{PEAK}$ exp [V]	$PDIV_{PEAK}$ est [V]	Error %
0.4	588.31	586.90	-0.24
0.6	586.90	608.11	+3.61
0.6*	766.50	752.36	-1.84
0.8	687.31	692.96	+0.82
1.0	695.79	724.08	+4.07
1.2	866.91	851.36	-1.79
1.8	903.68	865.50	**-4.22**
Average			**2.37**

TABLE 8. PDIV estimation with km_{max} at 25°C.

Wire [mm]	$PDIV_{PEAK}$ exp [V]	$PDIV_{PEAK}$ est [V]	Error %
0.4	588.31	615.18	+4.57
0.6	586.90	636.40	+8.43
0.6*	766.50	784.89	+2.40
0.8	687.31	726.91	+5.76
1.0	695.79	756.60	**+8.74**
1.2	866.91	886.71	+2.28
1.8	903.68	903.68	0.00
Average			**4.60**

The estimated voltages, in addition with the errors made are presented in Table 6, Table 7 and Table 8.

As expected, the average error is minimized when the average value of parameter k is used. As derived from the results, the use of one km from one wire can lead to errors up to 8.74% on PDIV estimation. On the contrary, the km characterization by means of several wires leads to errors below 5% and average errors are halved. The use of the extreme values almost duplicates the error. The use of $km_{\min}$ underestimates the PDIV, consequently, the insulation system designed would withstand greater voltage value without PD activity. On the contrary, using $km_{\max}$ overestimate the PDIV, resulting a risky insulation system not free of PD activity. To quantify the importance of these errors on PDIV estimation, some other sources of errors are going to be analysed in the next section. Previous works as [14], [15], [17] have given deviations between 6% to 12%.

In [14], the test object is a wire of diameter 0.71 mm and 44 μm of insulation thickness. Our closest wire of Table 1 is 0.6* mm with 30 μm of insulation thickness. In the study [15], the wire diameter is 1.25 mm with 40 μm of insulation thickness, close to the data of our 1.2 mm with 42 μm of insulation thickness. Comparing previous data from [14] and [15] with similar wire geometries, and naturally with [17], the predictions with km_{avg}, give similar magnitudes in terms of ionizing field in air (around 16 kV/mm).

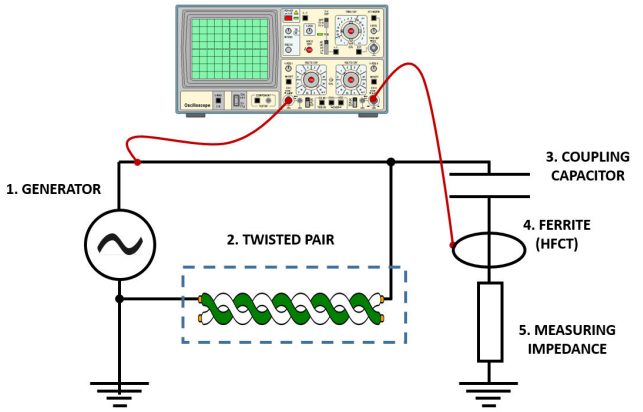

FIGURE 12. Test circuit components for instantaneous PDIV measurement in ϕ1.8 mm.

C. INFLUENCE OF ERRORS IN THE INSTANTANEOUS PDIV MEASUREMENT

The voltage measurements summarized in Table 2, Table 3 and Table 4 are calculated by multiplying by $\sqrt{2}$ the RMS values displayed on the generator. This is a quite common way to characterize PDIV, but the real instantaneous voltage value that triggers the partial discharge mechanism may differ slighty from the one obtained, due to the harmonic content of the applied wave.

The instantaneous PDIV voltage for 1.8 mm diameter magnet wire was measured using an oscilloscope connected as shown in Figure 12, with a sampling frequency of 50 MS/s on a 20 ms time window. The acquisition was configured in a single mode for the trigger to detect the first PD event from the increasing applied voltage. The Figure 13 shows different screenshots taken from the oscilloscope. These waveforms were stored and processed to calculate the accurate instantaneous applied voltage which created the PD event.

It is clear that, in general terms, the first partial discharge event is near the maximum (minimum) of the voltage wave. After 20 measurements and the Weibull fitting process, the PDIV instantaneous obtained is 991.45 V_{PEAK}, which results in an error of $+\mathbf{8.85\%}$ compared to that of Table 2. Thus, it is clear that the real PDIV value which ignites ionization can have deviations above those presented in Tables 6 to 8, so the errors from the model are not so high.

D. INFLUENCE OF ERRORS FROM MOISTURE

According to [22], [23], PDIV in dry air is higher than in moist air, due to the differences in the relative permittivity. This may lead to experimental deviations for temperatures below 100 °C. This effect was experienced when the environmental conditions were P=1015.6 hPa and RH=25.5%, a lower humidity value than all those shown in Table 2. We took this opportunity to measure again the PDIV of the 1.0 mm diameter wire under these environmental conditions. The experimental procedure was the same as that explained in Section II (10 samples).

The PDIV measured was 567 V_{RMS}. That represents 15% increment in the PDIV, thereby an increment in the parameter

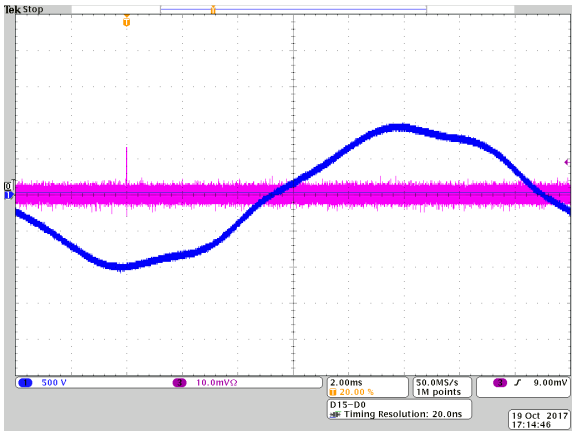

(a) ϕ 1.8 mm example #1

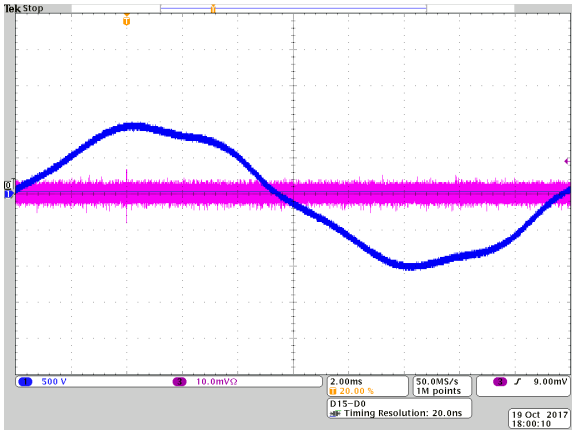

(b) ϕ 1.8 mm example #2

FIGURE 13. Examples of oscilloscope screenshots for cables with ϕ 1.8 mm.

k of this magnet wire (5.67 vs 4.55). This outlier value would increase the errors made by the model, because Paschen's Law does not consider the humidity effect.

E. MODEL PREDICTION FOR HIGH TEMPERATURE

The classical Paschen's Law is only valid for uniform fields and room temperature. To include the temperature effect in the PDIV, it is necessary to modelate the variation in the air density. The work [24] modifies the Equation 1, based on the Gay-Lussac Law (see Equation 7). The same formula was applied in [17] defining a corrected pressure value.

$$E = \frac{U}{d} = \frac{B \cdot P \cdot (\frac{273+25}{T+273})}{\ln\left(\frac{A \cdot P \cdot (\frac{273+25}{T+273}) \cdot d}{k}\right)} \tag{7}$$

This modification allows to apply the same process detailed in subsection VI-B, with km_{avg}=4.86 calculated for 25°C, to estimate the PDIV for higher temperatures. In this particular case, the results for 110°C and 150°C are presented in Table 9 and Table 10 respectively.

Using the parameter k obtained at 25°C to estimate PDIV at higher temperatures causes an increase in the error made by the model, even though the Equation 7 is taking into account the effect of temperature. This average error grows from 2.37% at 25°C to 5.22% at 110°C and 6.86% at 150°C. The maximum error value is 11.15%, slightly greater than the error introduced by the voltage generator. This results are similar to the ones presented in [17], with a maximum relative error of 9%.

TABLE 9. PDIV estimation with km_{avg} at 110°C.

Wire [mm]	$PDIV_{PEAK}$ exp [V]	$PDIV_{PEAK}$ th [V]	Error %
0.4	513	546	5.96
0.6	557	563	1.01
0.6*	701	679	-3.33
0.8	632	634	0.22
1.0	697	656	-6.25
1.2	830	758	-9.51
1.8	851	772	-10.26

TABLE 10. PDIV estimation with km_{avg} at 150°C.

Wire [mm]	$PDIV_{PEAK}$ exp [V]	$PDIV_{PEAK}$ th [V]	Error %
0.4	519.02	534.57	3.00
0.6	579.83	548.71	-5.37
0.6*	705.69	656.20	-7.01
0.8	649.12	616.60	-5.01
1.0	687.31	636.40	-7.41
1.2	824.49	732.56	-11.15
1.8	824.49	749.53	-9.09

TABLE 11. k parameter and γ for 25°C, 110°C and 150°C.

Temperature	k	γ
25 °C	4.86	0.0078
110 °C	5.11	0.0061
150 °C	5.34	0.0048

F. EXPERIMENTAL CALCULATION OF k FOR DIFFERENT TEMPERATURES

The results from subsection VI-E led us to study if the second ionzation coeficient has some dependence on temperature. This outcome is not surprising, because the Townsend's secondary emission coefficient γ is the average number of secondary electrons emitted from the cathode as a consequence of secondary ionization processes, which might be affected by thermo-ionic emission.

The calculation of parameter k detailed in subsection VI-A was performed at 110°C and 150°C using the Equation 7. The average value for these temperatures are $k = 5.11$ for 110°C and $k = 5.34$ for 150°C, greater than the $k = 4.86$ obtained for 25°C. These results show a growing trend of k with temperature.

A systematic process to calculate the Townsend's secondary emission coefficient γ is described, using Equation 6 and the k values. This methodology lead to the results of Table 11 and the spread of the γ calculated values is shown in Figure 14.

As opposed to parameter k, the Townsend's secondary emission coefficient γ shows a falling tendency with temperature, but the errors show a great overlap between the estimations, which means that the changes in epoxy resin type and in the manufacturer can be more important than those of temperature.

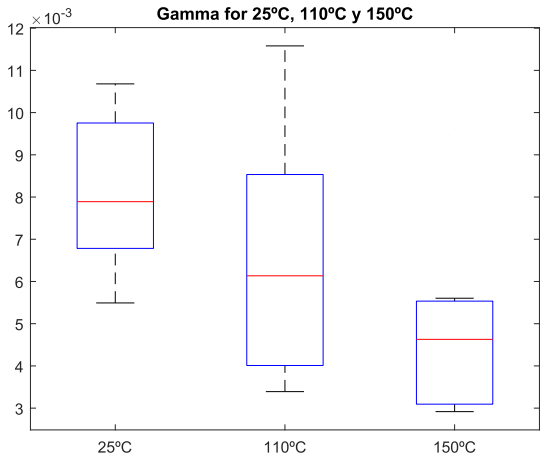

FIGURE 14. Parameter γ variation with the temperature.

VII. CONCLUSION

The proposed model based on Paschen's Law and Paschen's Law modified by Dunbar to include the temperature effect is a powerful tool for the design of insulation systems for new low-voltage motors. The process describes how to obtain the parameter k for ambient temperature, including an errors analysis of the variables which can influence and add uncertainty to the calculated value. This analysis allows a quantification of the parameter limits, to increase the risk level of the design if needed.

Despite the fact that there is an error interval for the PDIV prediction with the model, it is lower than those caused by real instantaneous PDIV measurement and environmental conditions. This uncertainty is created by the parameter k itself, which is not equal for all the wires analyzed. For this reason, the Townsend's secondary emission coefficient is an important source of error, so the authors have focused part of the work on its estimation.

The environmental conditions play a critical role in the partial discharge inception mechanism. Although the temperature and pressure are pretty well described by the Dunbar modification of Paschen's Law (Equation 7), the moisture of the air at room temperature is not taken into account and impact the results, creating errors with higher magnitudes than those from the prediction model.

Due to the increment in the temperature, the Townsend's secondary emission coefficient γ seems to be affected and thus the k parameter. When this happens, it is more likely for the electrons to reach enough energy to overcome the potential barrier and leave the surface. Therefore, the positive ion collision in the enamel at high temperature is more likely to lead to electron emission. However, the change on temperature is somehow hidden by the influence of enamel type (chemical composition) and wire manufacturer, which leads to great statistical dispersion on k calculation.

Thus, in this article the authors give the following main contributions:

1) Paschen's Law can be used to estimate PDIV with good accuracy for a wide range of temperatures if constant-field lines are used for the modelling.
2) Based on a study on 7 wires, gamma estimation for epoxy resin is 0.0078 at 25°C.
3) The use of gamma values from different wires can lead to errors up to 9% in PDIV estimation, so the type of epoxy resin greatly influences gamma.
4) Applied voltage harmonics lead to a deviation of PDIV higher than 8% compared to the use of RMS values.
5) Moisture also provokes some deviations in PDIV experimental data compared to that from the model below 100°C.
6) Gamma seems to decrease with temperature, but the trend is not so important compared to changes from the aforementioned magnitudes.

ACKNOWLEDGMENT

Tests have been made in the High-Voltage Research and Tests Laboratory (LINEALT), Universidad Carlos III de Madrid. The authors would like to thank Dr. Luca Lusuardi and Dr. Andrea Cavallini for their collaboration in this research.

REFERENCES

[1] S. Du, B. Wu, K. Tian, N. R. Zargari, and Z. Cheng, "An active cross-connected modular multilevel converter (AC-MMC) for a medium-voltage motor drive," *IEEE Trans. Ind. Electron.*, vol. 63, no. 8, pp. 4707–4717, Aug. 2016, doi: 10.1109/TIE.2016.2547875.

[2] P. A. Santos, J. A. T. Altuna, I. R. S. Casella, A. J. Sguarezi Filho, and C. E. Capovilla, "Overvoltage minimization in induction motors employing long cable PWM drives," *IEEE Latin Amer. Trans.*, vol. 13, no. 9, pp. 2895–2900, Sep. 2015, doi: 10.1109/TLA.2015.7350036.

[3] J. M. Martinez-Tarifa, H. Amaras-Duarte, and J. Sanz-Feito, "Frequency-domain model for calculation of voltage distribution through random wound coils and its interaction with stray capacitances," *IEEE Trans. Energy Convers.*, vol. 23, no. 3, pp. 742–751, Sep. 2008.

[4] J. M. Martínez-Tarifa, J. Sanz-Feito, and H. Amarís, "Reduction of electrical stresses on low-voltage induction motor insulation systems through remote-controlled inverters," *Electr. Power Compon. Syst.*, vol. 36, no. 9, pp. 885–896, Aug. 2008.

[5] P. Bidan, T. Lebey, G. Montseny, and J. Saint-Michel, "Transient voltage distribution in inverter fed motor windings: Experimental study and modeling," *IEEE Trans. Power Electron.*, vol. 16, no. 1, pp. 92–100, Jan. 2001, doi: 10.1109/63.903993.

[6] M. Kaufhold, G. Borner, M. Eberhardt, and J. Speck, "Failure mechanism of the interturn insulation of low voltage electric machines fed by pulse-controlled inverters," *IEEE Elect. Insul. Mag.*, vol. 12, no. 5, pp. 9–16, Sep. 1996, doi: 10.1109/57.537190.

[7] D. Fabiani, G. C. Montanari, and A. Contin, "Aging acceleration of insulating materials for electrical machine windings supplied by PWM in the presence and in the absence of partial discharges," in *Proc. IEEE 7th Int. Conf. Solid Dielectr.*, Jun. 2001, pp. 25–29.

[8] T. Billard, T. Lebey, and F. Fresnet, "Partial discharge in electric motor fed by a PWM inverter: Off-line and on-line detection," *IEEE Trans. Dielectr. Electr. Insul.*, vol. 21, no. 3, pp. 1235–1242, Jun. 2014.

[9] G. C. Stone, S. R. Campbell, and H. G. Sedding, "Analysis of the effect of adjustable speed drive surges on motor stator winding insulation," in *Proc. CIGRE Session*, 1998.

[10] M. Fenger, S. R. Campbell, and J. Pedersen, "Motor winding problems: Caused by inverter drives," *IEEE Ind. Appl. Mag.*, vol. 9, no. 4, pp. 22–31, Jul. 2003.

[11] Z. Xu, C. Hu, F. Yang, S.-H. Kuo, C.-K. Goh, A. Gupta, and S. Nadarajan, "Data-driven inter-turn short circuit fault detection in induction machines," *IEEE Access*, vol. 5, pp. 25055–25068, 2017.

[12] S. Kumar, D. Mukherjee, P. K. Guchhait, R. Banerjee, A. K. Srivastava, D. N. Vishwakarma, and R. K. Saket, "A comprehensive review of condition based prognostic maintenance (CBPM) for induction motor," *IEEE Access*, vol. 7, pp. 90690–90704, 2019.

[13] *Rotating Electrical Machines—Part 18-41: Partial Discharge Free Electrical Insulation Systems (Type I) Used in Rotating Electrical Machines Fed From Voltage Converters-Qualification and Quality Control Tests*, document IEC 60034-18-41, 2014.
[14] S. Duchesne, G. Parent, J. Moenecley, and D. Roger, "Prediction of PDIV in motor coils using finite element method," in *Proc. IEEE Int. Conf. Dielectr. (ICD)*, Jul. 2016, pp. 3–7.
[15] P. Rain, F. Loubeau, A. Durieux, F. Le Strat, and F. Fresnet, "Using motorettes for the experimental and numerical determinations of the PDIV in an electric motor," in *Proc. IEEE Int. Conf. Dielectr. (ICD)*, Jul. 2016, pp. 3–7.
[16] M. Szczepanski, D. Malec, P. Maussion, and P. Manfe, "Design of experiments predictive models as a tool for lifespan prediction and comparison for enameled wires used in low-voltage inverter-fed motors," *IEEE Trans. Ind. Appl.*, vol. 56, no. 3, pp. 3100–3113, May 2020, doi: 10.1109/TIA.2020.2970855.
[17] L. Lusuardi, A. Cavallini, M. G. de la Calle, J. M. Martinez-Tarifa, and G. Robles, "Insulation design of low voltage electrical motors fed by PWM inverters," *IEEE Elect. Insul. Mag.*, vol. 35, no. 3, pp. 7–15, May 2019.
[18] E. Kuffel, W. S. Zaengl, and J. Kuffel, *High Voltage Engineering Fundamentals*. Oxford, U.K.: Newnes, 2000.
[19] N. Malik, "Streamer breakdown criterion for compressed gases," *IEEE Trans. Electr. Insul.*, vol. EI-16, no. 5, pp. 463–467, Oct. 1981.
[20] P. G. Slade and E. D. Taylor, "Electrical breakdown in atmospheric air between closely spaced (0.2 μm–40 μm) electrical contacts," *IEEE Trans. Compon. Packag. Technol.*, vol. 25, no. 3, pp. 390–396, Sep. 2002.
[21] C. Pan, J. Tang, Y. Zhang, X. Luo, and X. Li, "Variation of discharge characteristics with temperature in moving transformer oil contaminated by metallic particles," *IEEE Access*, vol. 6, pp. 40050–40058, 2018.
[22] Z. Nawawi, Y. Muramoto, N. Hozumi, and M. Nagao, "Effect of humidity on partial discharge characteristics," in *Proc. 7th Int. Conf. Properties Appl. Dielectric Mater.*, Nagoya, Japan, vol. 1, 2003, pp. 307–310.
[23] P. Wang, Y. Gu, Q. Wu, A. Cavallini, Q. Zhang, J. Zhang, P. Li, and Y. Li, "Influence of ambient humidity on PDIV and endurance of inverter-fed motor insulation," in *Proc. IEEE Electr. Insul. Conf. (EIC)*, Calgary, AB, Canada, Jun. 2019, pp. 201–204, doi: 10.1109/EIC43217.2019.9046593.
[24] B. Dobbs, W. G. Dunbar, and C. Tarvin, "High voltage design guide summary," in *Proc. 24th Intersociety Energy Convers. Eng. Conf.*, Washington, DC, USA, vol. 1, 1989, pp. 423–428, doi: 10.1109/IECEC.1989.74497.

MANUEL GÓMEZ DE LA CALLE was born in Segovia, Spain, in 1987. He received the Industrial Engineering degree (major in electronics) from Universidad Pontificia Comillas (ICAI), Madrid, Spain, in 2010. He is currently pursuing the Ph.D. degree in electrical engineering, electronics and automation with the Universidad Carlos III de Madrid. In September 2018, he joined the Departamento de Ingeniería Eléctrica, Universidad Pontificia Comillas (ICAI), as a part-time Professor for the Electrical Machines Laboratory. He is also with the Electrical Design Office Department, Airbus Defence and Space, Madrid, where he is working in the protection system for the new high voltage aeronautical architectures. His research interests include the reliability of electrical systems fed by PWM inverters, partial discharge measurements at different voltages and environmental conditions, and electric arcs in direct current networks.

JUAN MANUEL MARTÍNEZ-TARIFA (Senior Member, IEEE) was born in Lorca, Spain, in 1975. He received the M.Sc. degree in electronic engineering and the M.Sc. degree in physics from the Universidad de Granada, Spain, in 1999 and 2000, respectively, and the Ph.D. degree in electrical engineering from the Universidad Carlos III de Madrid (UC3M), Spain, in 2005. From 2000 to 2012, he was an Assistant Professor with the Department of Electrical Engineering, UC3M, where he is currently an Associate Professor. He is also the Supervisor with the High-Voltage Research and Tests Laboratory (LINEALT), UC3M, where he is working on the diagnosis of insulation systems within power cables and electrical machines. He has published over 60 papers in international journals and conferences. He has joined several research teams to work in over ten research projects financed by public and private funds.

ÁNGEL MANUEL GÓMEZ SOLANILLA was born in Ciudad Real, Spain, in 1978. He received the Technical Engineering degree (major in electrical) and the Industrial Engineering degree from Universidad de Castilla-La Mancha (UCLM), Spain, in 2001 and 2015, respectively. In 2001, he joined the Department of Electrical Engineering, Universidad Carlos III de Madrid (UC3M), where he is currently a Laboratory Technician specialized in electrical tests and collaborates with the High-Voltage Research and Tests Laboratory (LINEALT).

GUILLERMO ROBLES (Senior Member, IEEE) was born in Madrid, Spain, in 1969. He received the M.Sc. and Ph.D. degrees in electronic engineering from Universidad Pontificia Comillas, Madrid, in 1993 and 2002, respectively. He is currently with the Department of Electrical Engineering, Universidad Carlos III de Madrid (UC3M), Madrid, where he has been an Associate Professor, since 2009. He is also with the High-Voltage Research and Tests Laboratory (LINEALT), UC3M. He has coauthored more than 90 papers in international journals and conferences in the areas of sensor design, signal processing, instrumentation, and measurement focused especially on the diagnosis of insulation systems of electrical machines. His research interest includes the design and development of energy harvesting systems based on piezoelectrics, thermoelectric, and electromagnetic generators. He is an Associate Editor of the IEEE TRANSACTIONS ON DIELECTRICS AND ELECTRICAL INSULATION and a Guest Editor of *Sensors*—MDPI.